Cardiovascular Research (2010) **85**, 376–384
doi:10.1093/cvr/cvp344

Proteomic remodelling of mitochondrial oxidative pathways in pressure overload-induced heart failure

Heiko Bugger[2†], Michael Schwarzer[1], Dong Chen[4], Andrea Schrepper[1], Paulo A. Amorim[1], Maria Schoepe[1], T. Dung Nguyen[1], Friedrich W. Mohr[1], Oleh Khalimonchuk[3], Bart C. Weimer[4‡], and Torsten Doenst[1*]

[1]Department of Cardiac Surgery, University of Leipzig Heart Center, Strümpellstr. 39, Leipzig 04289, Germany; [2]Program in Molecular Medicine and Division of Endocrinology, Metabolism and Diabetes, Salt Lake City, UT, USA; [3]Department of Biochemistry, University of Utah School of Medicine, Salt Lake City, UT, USA; and [4]Department of Nutrition and Food Sciences and Center for Integrated BioSystems, Utah State University, Logan, UT, USA

Received 18 June 2009; revised 3 October 2009; accepted 12 October 2009; online publish-ahead-of-print 19 October 2009

Time for primary review: 42 days

Aims Impairment in mitochondrial energetics is a common observation in animal models of heart failure, the underlying mechanisms of which remain incompletely understood. It was our objective to investigate whether changes in mitochondrial protein levels may explain impairment in mitochondrial oxidative capacity in pressure overload-induced heart failure.

Methods and results Twenty weeks following aortic constriction, Sprague-Dawley rats developed contractile dysfunction with clinical signs of heart failure. Comparative mitochondrial proteomics using label-free proteome expression analysis (LC-MS/MS) revealed decreased mitochondrial abundance of fatty acid oxidation proteins (six of 11 proteins detected), increased levels of pyruvate dehydrogenase subunits, and upregulation of two tricarboxylic acid cycle proteins. Regulation of mitochondrial electron transport chain subunits was variable, with downregulation of 53% of proteins and upregulation of 25% of proteins. Mitochondrial state 3 respiration was markedly decreased independent of the substrate used (palmitoyl-carnitine −65%, pyruvate −75%, glutamate −75%, dinitrophenol −82%; all $P < 0.05$), associated with impaired mitochondrial cristae morphology in failing hearts. Perfusion of isolated working failing hearts showed markedly reduced oleate (−68%; $P < 0.05$) and glucose oxidation (−64%; $P < 0.05$).

Conclusion Pressure overload-induced heart failure is characterized by a substantial defect in cardiac oxidative capacity, at least in part due to a mitochondrial defect downstream of substrate-specific pathways. Numerous changes in mitochondrial protein levels have been detected, and the contribution of these to oxidative defects and impaired cardiac energetics in failing hearts is discussed.

Keywords Chronic heart failure • Pressure overload • Metabolism • Mitochondria • Proteomic remodelling

1. Introduction

Mitochondrial oxidation of energy substrates is the main source of high energy phosphates for cardiac contractile function. Impairment in mitochondrial function is thought to contribute to mechanical dysfunction in numerous cardiac disease states, including heart failure.[1–3] However, the underlying mechanisms for mitochondrial dysfunction in heart failure are incompletely understood, which is partially due to the use of animal models with different aetiologies of heart failure (ischaemia-induced vs. pacing-induced

†Present address. Department of Cardiology, University of Freiburg, Freiburg, Germany.

‡Present address. Department of Population Health and Reproduction, University of California, Davis, School of Veterinary Medicine, Davis, CA, USA.

* Corresponding author. Tel: +49 341 865 1423, Fax: +49 341 865 1452, Email: torsten.doenst@med.uni-leipzig.de

vs. hypertension-induced), and variations in the severity of heart failure (early vs. late stage disease). Proposed mechanisms for mitochondrial dysfunction include impairment in electron transport chain (ETC) complex activities,[4] defects in supermolecular assembly of ETC complexes,[2] oxidative stress,[5,6] decreases in mitochondrial membrane tetralinoleoyl cardiolipin content,[7] impaired tricarboxylic acid (TCA) cycle anaplerosis,[8] and mitochondrial uncoupling.[9]

A common cause of heart failure is chronic pressure overload due to hypertension or aortic stenosis, which leads to cardiac hypertrophy that may progress to heart failure. Microarray analyses in hypertrophied hearts suggest that alterations in myocardial substrate oxidation following pressure overload are determined by changes in gene expression.[10,11] Indeed, several studies have shown that mRNA expression of fatty acid oxidation (FAO) genes is reduced in pressure overload-induced hypertrophy, associated with reduced rates of cardiac FAO.[12–14] Only few studies have investigated the contribution of changes in gene expression to altered cardiac energy metabolism when pressure overload-induced hypertrophy progresses to overt heart failure. Garnier *et al.*[4] showed that gene expression of the transcriptional coactivator PGC-1α and its target gene cytochrome *c* oxidase subunit 4 (COX4) are decreased, associated with decreased activity of cytochrome *c* oxidase activity, suggesting that mitochondrial oxidative defects may partially result from transcriptional downregulation of ETC subunits, although mitochondrial protein levels were not evaluated in this study. Thus far, it remains incompletely understood whether substrate metabolic adaptation and impairment in mitochondrial respiratory function in the model of pressure overload-induced heart failure are indeed a direct consequence of changes in gene and consecutive protein expression, or whether post-translational mechanisms play a decisive role.

Protein profiling has emerged as a powerful tool to survey the protein composition of cells or cell organelles.[15–18] In particular, analyses of the mitochondrial proteome have improved our understanding of this complex organelle and its manifold functions in cellular biology.[16,17,19] Mitochondrial proteomics provides a unique opportunity to simultaneously measure mitochondrial protein levels of many metabolic enzymes in a single assay. Recent studies using mitochondrial comparative proteomics provided insight into the mechanisms of cardiac mitochondrial dysfunction in mice with cardiomyocyte-restricted deletion of the insulin receptor (CIRKO mice) and diabetes-associated defects in mitochondrial energetics of Type 1 diabetic Akita mice.[1,20]

In the present study, we hypothesized that changes in mitochondrial protein levels contribute to mitochondrial oxidative dysfunction in pressure overload-induced heart failure. To test this hypothesis, we characterized the cardiac mitochondrial proteome in rats developing heart failure following chronic pressure overload using label-free proteome expression analysis and combined this proteomic survey with measurements of gene expression, mitochondrial respiration rates, and whole heart substrate oxidation. Our proteomic approach identified downregulation of FAO enzymes, upregulation of pyruvate dehydrogenase (PDH) subunits, and numerous bidirectional changes in ETC subunit composition. This remodelling of the mitochondrial proteome was associated with severe defects in mitochondrial and whole heart oxidative capacity. The potential contribution of mitochondrial proteomic remodelling to impaired cardiac energetics in pressure overload-induced heart failure is discussed.

2. Methods

2.1 Animals

Male Sprague-Dawley rats (40–50 g) were obtained from Charles River (Sulzfeld, Germany) and were fed *ad libitum* at 21°C with a light cycle of 12 h. The use of animals and the experimental protocols were approved by the local Animal Welfare Committees (Reg-Präs Freiburg G-05/55, Landesdirektion Leipzig TVV 36/06). The investigation conforms with the Guide for the Care and Use of Laboratory Animals published by the US National Institutes of Health (NIH Publication No. 85-23, revised 1996).

2.2 Surgical interventions

Heart failure was induced by transverse aortic constriction as essentially described before.[21] In brief, rats (40–50 g) were anaesthetized with intraperitoneal ketamine (50 mg/kg) and xylazine (10 mg/kg), and a tantalum clip (0.35 mm internal diameter; Pilling-Weck, Kernen, Germany) was placed on the aorta between the brachiocephalic trunk and the left common carotid artery. Animals were sacrificed 20 weeks following aortic constriction. Age-matched sham-operated animals underwent the same procedure, without clip application.

2.3 Echocardiography

Animals were anaesthetized with Fentanyl/Midazolamhydrochlorid/Medetomidinhydrochlorid (0.005/2/0.15 mg/kg). Rats were examined in supine position with a 7 MHz phased array transducer (Agilent/Philipps, Germany). Two-dimensional short-axis views of the left ventricle at papillary muscle level were obtained, and two-dimensional guided M-mode tracings were recorded with a sweep speed of 100 mm/s.

2.4 Isolated working heart perfusion

Hearts were perfused in the isolated working mode as described before,[22] using Krebs-Henseleit buffer containing 5 mM glucose and 0.4 mM Na-oleate. All experiments were carried out with a preload of 15 cm H_2O and an afterload of 100 cm H_2O. Glucose and oleate oxidation were determined from the production of $^{14}CO_2$ and ^3H_2O, respectively, using [U-^{14}C] glucose and [9,10-^{3}H] oleate as tracer substrates.

2.5 Isolation of mitochondria and mitochondrial membranes

Hearts were freshly excised, and mitochondria were isolated by differential centrifugation. For details see Supplementary material online. Mitochondrial membrane fractions for mitochondrial proteomics were generated as described before.[1]

2.6 Mitochondrial respiration

Mitochondrial oxygen consumption was measured in a 1 mL water-jacketed respiration chamber (25°C) using a Clark-type oxygen electrode (Strathkelvin, Scotland). Respiration was measured in respiration medium (100 mM KCl, 50 mM Mops, 1 mM EGTA, 5 mM KH_2PO_4, 1 mg/mL BSA, pH 7.4) containing 10 mM glutamate, 20 μM palmitoylcarnitine/2.5 mM malate, or 5 mM pyruvate/2.5 mM malate. State 3 respiration was recorded following addition of 1 mM adenosine diphosphate (ADP), and state 4 respiration following complete phosphorylation of the added ADP. To measure dinitrophenol-stimulated

respiration, state 2 was measured in the presence of 10 mM glutamate, and state 3 following addition of 0.1 mM dinitrophenol. Protein content was determined using the Bradford method.

2.7 Electron microscopy

Left ventricular samples were taken from freshly excised hearts, washed, fixed in 2.5% glutaraldehyde/1% paraformaldehyde, post-fixed in 2% osmium tetroxide, embedded in resin, and sectioned. Mitochondrial volume density and number were quantified by stereology in a blinded fashion using the point counting method.[23] Changes in mitochondrial cristae morphology were quantified by counting mitochondria with reduced lamellar density (<50% of normal lamellar density) and/or abnormal lamellar structure, and by expressing these mitochondria relative to the total number of mitochondria counted.

2.8 Quantitative real-time PCR

Myocardial mRNA was extracted from snap-frozen tissue samples using the Qiagen RNeasy Mini Kit. Synthesis of complementary DNA was performed with the cDNA synthesis kit from Fermentas (St Leon-Rot, Germany), and TaqMan quantitative real-time RT–PCR was performed using Ampli *Taq* Gold (ABI) with the conditions suggested by the manufacturer on the ABI 7900 HT, as essentially described before.[24,25] Forward and reverse primers were designed using the Universal Probe Library Assay Design Centre. For each set of primers, a basic local alignment search tool (BLAST) search revealed that sequence homology was obtained only for the target gene. Amplification was allowed to proceed for 40 cycles, and a series of five dilutions was analysed for each target gene to construct standard curves. Results were normalized to the invariant transcript S29 ribosomal protein and are presented as fold change compared with sham, which was set to one. Primer and probe sequences are shown in Supplementary material online, *Table S1*.

2.9 Mitochondrial protein identification and quantification by LC-MS/MS

Isolated mitochondria or mitochondrial membranes were tryptically digested according to a modified digestion method in the Waters Protein Expression System Manual (Waters, 2006), as described before.[1] Digested protein samples were introduced into a Symmetry® C18 trapping column by NanoACQUITY Sample Manager (Waters, Manchester, UK), eluted using an NanoACQUITY UPLC (Waters), and introduced into a Q-TOF Premier mass spectrometer (Waters). Mass spectrometry data were analysed using Waters ProteinLynx Global Server (PLGS) 2.3. Canonical pathway analysis was performed using the Ingenuity Pathways Analysis (IPA) software (Redwood City, CA, USA). For further details, see Supplementary material online.

2.10 Statistical analysis

Data are presented as mean ± SEM. Data were analysed using a Student's *t*-test using the Sigma Stat 3.1 software package. Proteomic data were analysed using Water ProteinLynx Global Server (PLGS) 2.3. Differences among groups were considered statistically significant if $P < 0.05$.

3. Results

3.1 Aortic constriction causes heart failure

Twenty weeks following surgery, heart weights and heart weight-to-tibia length ratios were increased in rats with aortic constriction compared with sham-operated rats (*Table 1*). Lung weight-to-body weight ratios were also increased, indicating pulmonary congestion (*Table 1*). Echocardiography showed increased interventricular septum diameter, left ventricular posterior wall thickness, and left ventricular end-systolic and end-diastolic diameter (*Table 2*). Ejection fraction and fractional shortening were significantly reduced by 29 and 36% in rats following aortic constriction, respectively, indicating systolic dysfunction (*Table 2*). Mortality following surgery was higher in animals receiving aortic constriction compared with sham-operated rats (see Supplementary material online, *Figure S1*). Thus, rats developed heart failure following aortic constriction and will be referred to as failing hearts in this manuscript.

3.2 Remodelling of the mitochondrial proteome in failing hearts

Abundance of mitochondrial proteins was investigated by comparative mitochondrial proteomics using isolated mitochondria. Possible differences in the abundance of ETC subunits were investigated by the same proteomic analysis using mitochondrial membranes only

Table 1 Increased heart size in rats with aortic constriction

	Sham	Aortic constriction
Heart weight (g)	1.29 ± 0.05	2.53 ± 0.09*
Tibia length (mm)	41.0 ± 0.4	41.2 ± 0.4
Heart weight–tibia length ratio (mg/mm)	31.5 ± 1.3	61.4 ± 7.5*
Body weight (g)	408 ± 6	431 ± 15
Lung weight–body weight ratio (mg/g)	3.8 ± 0.1	9.9 ± 3.8*

Heart weight-to-tibia length ratios and lung weight-to-body weight ratios of sham-operated rats ($n = 27$) and rats with aortic constriction ($n = 9$).
*$P < 0.05$ vs. Sham.

Table 2 Rats with aortic constriction develop heart failure

	Sham	Aortic constriction
IVSS (mm)	2.9 ± 0.1	3.5 ± 0.2*
IVSD (mm)	1.7 ± 0.1	2.5 ± 0.2*
LVESD (mm)	4.3 ± 0.1	6.3 ± 0.2*
LVEDD (mm)	7.5 ± 0.1	8.6 ± 0.3*
LVPWS (mm)	3.0 ± 0.1	3.7 ± 0.2*
LVPWD (mm)	1.9 ± 0.1	3.1 ± 0.2*
EF (%)	70.9 ± 1.1	50.3 ± 2.0*
FS (%)	41.9 ± 0.9	26.9 ± 1.3*

Echocardiographic measurement of morphometric and contractile parameters of sham-operated rats ($n = 27$) and rats with aortic constriction ($n = 9$).
*$P < 0.05$ vs. Sham.

Table 3 Downregulation of FAO proteins in failing hearts

Protein	Fold change
Fatty acid oxidation	
Acetyl-coenzyme A acyltransferase 2 (mitochondrial 3-oxoacyl-coenzyme A thiolase)	0.89
Acetyl-coenzyme A dehydrogenase, long-chain	1.14*
Acetyl-coenzyme A dehydrogenase, medium chain	0.77*
Acyl-coenzyme A dehydrogenase, short chain	0.77*
Acyl-coenzyme A dehydrogenase, very long chain	0.75*
Dodecenoyl-coenzyme A delta isomerase	0.86
Enoyl coenzyme A hydratase, short chain, 1, mitochondrial	1.09
Hydroxysteroid (17-beta) dehydrogenase 10	0.90
L-3-hydroxyacyl-coenzyme A dehydrogenase	0.57*
Mitochondrial trifunctional protein, alpha subunit	0.80*
Mitochondrial trifunctional protein, beta subunit	0.80*
Glucose oxidation	
Dihydrolipoamide dehydrogenase (E3 component of pyruvate dehydrogenase complex, 2-oxo-glutarate complex, branched chain keto acid dehydrogenase complex)	1.25*
Dihydrolipoamide *S*-acetyltransferase (E2 component of pyruvate dehydrogenase complex)	1.60*
Pyruvate dehydrogenase (lipoamide) beta	1.25*
Citric acid cycle	
Aconitase 2, mitochondrial	1.21*
Citrate synthase	0.98
Fumarate hydratase 1	1.07
Malate dehydrogenase, mitochondrial	1.05
Succinate dehydrogenase complex, subunit A, flavoprotein	1.20*
Succinate-CoA ligase, GDP-forming, alpha subunit	0.99

Abundance of selected energy metabolic proteins detected in mitochondria isolated from hearts of sham-operated rats and rats with heart failure, presented as fold change compared with sham-operated animals.
*$P < 0.05$ vs. sham-operated.

(generated from the same mitochondrial isolate) to increase coverage of ETC subunits. Our proteomic approach resulted in the confident detection of 141 mitochondrial proteins in isolated mitochondria, 70 of which were significantly regulated in failing hearts compared with shams. In mitochondrial membranes, 174 proteins were detected, 123 of which showed significant changes compared with sham-operated animals. Proteins were sorted by canonical pathways using IPA software, and selected proteins are presented in *Tables 3* and *4*. The complete list of detected proteins is presented in Supplementary material online, *Tables S2* and *S3*.

Abundance of FAO proteins was generally reduced (six of 11 proteins detected) in mitochondria of failing hearts (*Table 3*). In contrast, protein components of the PDH complex were significantly upregulated. Two of six TCA cycle enzymes detected, mitochondrial aconitase and succinate dehydrogenase complex, subunit A, flavoprotein were also upregulated in mitochondria of failing hearts. As shown in *Table 4*, we identified 40 ETC subunits, 31 of which showed significantly different abundance in mitochondrial membranes of failing hearts. Of these 31 regulated ETC proteins, 21 proteins were significantly less abundant in membranes of failing hearts. Specifically, 10 subunits of complex I, three subunits of complex III, five subunits of complex IV, and three subunits of complex V were downregulated in mitochondrial membranes of failing hearts. Ten ETC subunits were significantly more abundant in mitochondrial membranes of failing hearts, some of which showed dramatic increases in abundance compared with shams (1.3 to 10.4-fold). Specifically, four subunits of complex I, one subunit of complex II, and five subunits of complex V were upregulated.

3.3 Mitochondrial dysfunction in failing hearts

Mitochondrial function of failing hearts was characterized by measuring mitochondrial respiration rates in isolated mitochondria using palmitoyl-carnitine, pyruvate, and glutamate as substrates. Protein yield of mitochondrial isolates obtained from failing hearts was significantly lower compared with shams (4.6 ± 0.3 vs. 9.0 ± 0.8 mg/g wet weight; $P<0.05$). State 3 respiration was markedly impaired in mitochondria obtained from failing hearts for all substrates tested (*Figure 1A–C*). State 3 respiration was also impaired to a similar extent using the uncoupling agent dinitrophenol in the presence of glutamate (*Figure 1D*). State 4 respirations were not different between failing hearts and shams for any substrate. ADP/O ratios were unchanged between the groups with pyruvate and glutamate, but were reduced with palmitoyl-carnitine as a substrate (*Figure 1E*).

3.4 Cardiac ultrastructure

Mitochondrial morphology and content were evaluated by electron microscopy (*Figure 2A*). As shown in *Figure 2B*, 34% of mitochondria showed dysorganized cristae and/or reduced cristae density in failing hearts, whereas only 8% of mitochondria showed morphological alterations in shams. Stereological quantification revealed a slight but significant decrease in mitochondrial volume density in failing hearts (*Figure 2C*), whereas mitochondrial number was not different between groups (see Supplementary material online, *Figure S2*).

3.5 Impaired myocardial substrate oxidation in failing hearts

Mitochondrial dysfunction may limit myocardial oxidative capacity and contractile function. We therefore measured myocardial substrate oxidation and contractile performance in the isolated working heart. Cardiac power was markedly reduced in failing hearts (*Figure 3A*). Both oxidation of oleate and glucose were markedly reduced by 68 and 64% in failing hearts, respectively (*Figure 3B* and *C*). Interestingly, oleate and glucose oxidation were reduced to similar extents, thus the ratio of glucose oxidation to oleate oxidation was unchanged (*Figure 3D*).

3.6 Gene expression in failing hearts

Figure 4A shows the expression of genes encoding for ETC subunits, for transcription factors and transcriptional coactivators of mitochondrial biogenesis, and for proteins of fatty acid and glucose utilization. Expression of the ETC subunits Ndufa9, Sdhb, and COX5b

Table 4 Downregulation of OXPHOS proteins in failing hearts

Protein	Fold change
OXPHOS complex I	
NADH dehydrogenase (ubiquinone) 1 alpha subcomplex 10	1.80*
NADH dehydrogenase (ubiquinone) 1 beta subcomplex, 4, 15 kDa	3.82*
NADH dehydrogenase (ubiquinone) 1, subcomplex unknown, 2	1.12
NADH dehydrogenase (ubiquinone) Fe–S protein 1, 75 kDa	0.84*
NADH dehydrogenase (ubiquinone) Fe–S protein 2	0.85*
NADH dehydrogenase (ubiquinone) Fe–S protein 4, 18 kDa	0.91
NADH dehydrogenase (ubiquinone) Fe–S protein 7	0.76*
NADH dehydrogenase (ubiquinone) flavoprotein 1, 51 kDa	0.8*
NADH dehydrogenase (ubiquinone) flavoprotein 2	0.88*
NADH dehydrogenase 1 alpha subcomplex 10-like protein	1.73*
PREDICTED: NADH dehydrogenase (ubiquinone) Fe-S protein 6	0.90
PREDICTED: similar to NADH dehydrogenase (ubiquinone) 1 alpha subcomplex, 13	0.79*
PREDICTED: similar to NADH dehydrogenase (ubiquinone) 1 alpha subcomplex, 2	0.74*
PREDICTED: similar to NADH dehydrogenase (ubiquinone) 1 alpha subcomplex, 9	0.79*
PREDICTED: similar to NADH dehydrogenase (ubiquinone) 1 beta subcomplex, 5	0.82*
PREDICTED: similar to NADH dehydrogenase (ubiquinone) 1 beta subcomplex, 7	0.79
PREDICTED: similar to NADH dehydrogenase (ubiquinone) Fe–S protein 3	0.8*
PREDICTED: similar to NADH-ubiquinone oxidoreductase ESSS subunit	0.82
PREDICTED: similar to NADH-ubiquinone oxidoreductase MLRQ subunit	1.34*
OXPHOS complex II	
Succinate dehydrogenase complex, subunit A, flavoprotein	1.58*
OXPHOS complex III	
PREDICTED: similar to ubiquinol-cytochrome *c* reductase binding protein	0.48*
Ubiquinol-cytochrome *c* reductase core protein I	0.87*
Ubiquinol-cytochrome *c* reductase core protein II	0.90*
ubiquinol-cytochrome *c* reductase, Rieske iron-sulfur polypeptide 1	0.92
OXPHOS complex IV	
Cytochrome *c* oxidase subunit II	0.79*
Cytochrome *c* oxidase subunit IV isoform 1	0.79*
Cytochrome *c* oxidase subunit Vb	0.84*
Cytochrome *c* oxidase, subunit 7a 3	0.83*
Cytochrome *c* oxidase, subunit Va	0.92
PREDICTED: similar to cytochrome *c* oxidase subunit VIIa polypeptide 2-like	1.04
PREDICTED: similar to cytochrome *c* oxidase, subunit 7a 3	0.82*
OXPHOS complex V	
ATP synthase, H+ transporting, mitochondrial F0 complex, subunit b, isoform 1	0.87*
ATP synthase, H+ transporting, mitochondrial F0 complex, subunit d	1.09
ATP synthase, H+ transporting, mitochondrial F0 complex, subunit E	0.80*
ATP synthase, H+ transporting, mitochondrial F0 complex, subunit F6	1.26*
ATP synthase, H+ transporting, mitochondrial F0 complex, subunit G	0.79*
ATP synthase, H+ transporting, mitochondrial F1 complex, alpha subunit, isoform 1	3.25*
ATP synthase, H+ transporting, mitochondrial F1 complex, beta subunit	10.38*
ATP synthase, H+ transporting, mitochondrial F1 complex, gamma subunit	3.46*
Mitochondrial ATP synthase, O subunit	1.55*

Abundance of OXPHOS subunits detected in mitochondrial membranes isolated from hearts of sham-operated rats and rats with heart failure, presented as fold change compared with sham-operated animals.
*$P < 0.05$ vs. sham-operated.

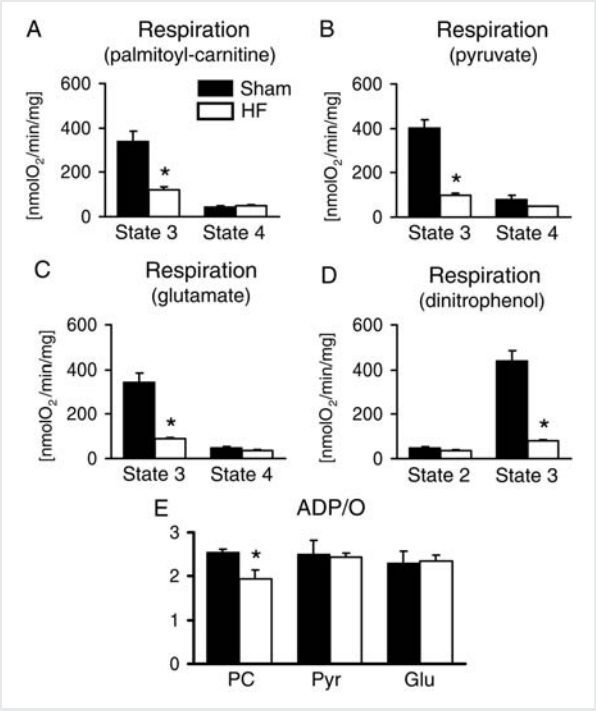

Figure 1 Mitochondrial dysfunction in failing hearts. State 3 and state 4 respiration rates with palmitoyl-carnitine or pyruvate or glutamate as substrates (*A*–*C*), respirations in the absence (state 2) and presence (state 3) of dinitrophenol (*D*), and ADP/O ratios (*E*) of mitochondria isolated from hearts of sham-operated rats (black bars, $n = 6$) and rats with heart failure (white bars; $n = 9$). PC, palmitoyl-carnitine; Pyr, pyruvate; Glu, glutamate. $^*P < 0.05$.

was reduced in failing hearts, whereas expression of Ndufs7, Uqcrc-1, Uqcrc-2, Uqcrbl, and COXIV was unchanged. Messenger RNA content of PGC-1α and ERRα was decreased, whereas expression of PGC-1β and NRF2 was increased. Expression of the FAO genes CPT1b and MCAD was reduced, whereas PPARα transcript levels were unchanged. Expression of PDK4 and GLUT4 was reduced, whereas GLUT1 expression was unaltered. When directly comparing the expression of ETC genes with respective protein levels from our proteomic survey, the magnitude of changes in mitochondrial ETC protein levels was less pronounced than on the mRNA level (*Figure 4B*). In addition, some ETC genes showed a clear trend towards up- or downregulation that was not identically displayed on the protein level.

4. Discussion

Transcriptional mechanisms have been implicated in the adaptations of the heart to chronic pressure overload, including changes in myocardial substrate oxidation.[10,12,13,26] Studies have shown that reduced FAO rates in pressure overload hypertrophy may result from downregulation of FAO genes and that impairment in mitochondrial function in pressure overload-induced heart failure may result from transcriptional downregulation of ETC genes.[4,12–14] In the present study, we evaluated the contribution of changes in mitochondrial protein abundance to alterations in substrate oxidation and mitochondrial respiratory dysfunction in pressure overload-induced heart failure using comparative mitochondrial proteomics. Mitochondrial respiratory capacity and whole heart oxidative capacity were severely depressed in failing hearts, both with substrates of fatty acid and carbohydrate oxidation. Our proteomic survey suggests that a general downregulation of FAO proteins in mitochondria of failing hearts contributes to reduced FAO rates, whereas the moderate extent and bidirectional regulation of changes in ETC subunit levels suggests that changes in ETC protein levels may only partially explain the severe defect in respiratory function in failing hearts.

Reduced expression of FAO genes, likely mediated by reduced signalling via PPARα, is held responsible for the downregulation of FAO rates following chronic pressure overload.[13,27] Our finding of reduced FAO protein levels in mitochondria of failing hearts strengthens this concept. In contrast, the pronounced defects in both fatty acid and glucose oxidative capacity in failing hearts in this study suggest additional mechanisms to occur and to contribute to both oxidative impairment and severe contractile deficits following transition of compensated hypertrophy to heart failure. The moderately pronounced downregulation of FAO proteins does not appear to fully explain the strong reduction in FAO rates in failing hearts and cannot explain why glucose oxidation was also markedly impaired in this setting. In addition, respiratory rates were markedly impaired, not only with fatty acids and carbohydrates as substrates but also with glutamate, thereby localizing the mitochondrial respiratory defect downstream of substrate-specific pathways, i.e. in the TCA cycle and/or ETC. Interestingly, mitochondrial respiratory function appears unaffected during compensated hypertrophy.[10] Thus, it appears that during compensated cardiac hypertrophy, transcriptional downregulation may limit FAO capacity, but after transition to overt heart failure, overall oxidative metabolism seems to be compromised, likely due to an additional mitochondrial respiratory defect downstream of substrate-specific pathways, as was recently proposed by Neubauer.[28]

More than 50% of ETC proteins were less abundant in mitochondria of failing hearts. Thus, reduced mitochondrial ETC protein levels may contribute, at least in part, to impaired respiratory function. The threshold below which a reduction in protein abundance translates into functional changes is unknown, but a decrease of 30% in enzyme content is considered to be functionally relevant, and several ETC subunits were 20–30% less abundant in failing hearts in the present study.[19] In addition, deletion or mutation of only a single ETC subunit can be sufficient to impair mitochondrial electron transport.[29,30] In how far the coexisting increased abundance of some ETC subunits will affect overall electron transport remains unclear and is difficult to evaluate. It could be speculated that a dysbalance of ETC subunits would also compromise optimal efficiency of electron transport with the result of impaired respiratory capacity and/or increased superoxide production.

Studies over the last few years suggest a role for the transcriptional coactivator and master regulator of mitochondrial biogenesis, PGC-1α, in the regulation of mitochondrial oxidative capacity in response to pressure overload.[31] Knockout of PGC-1α leads to downregulation of ETC genes in the heart, and

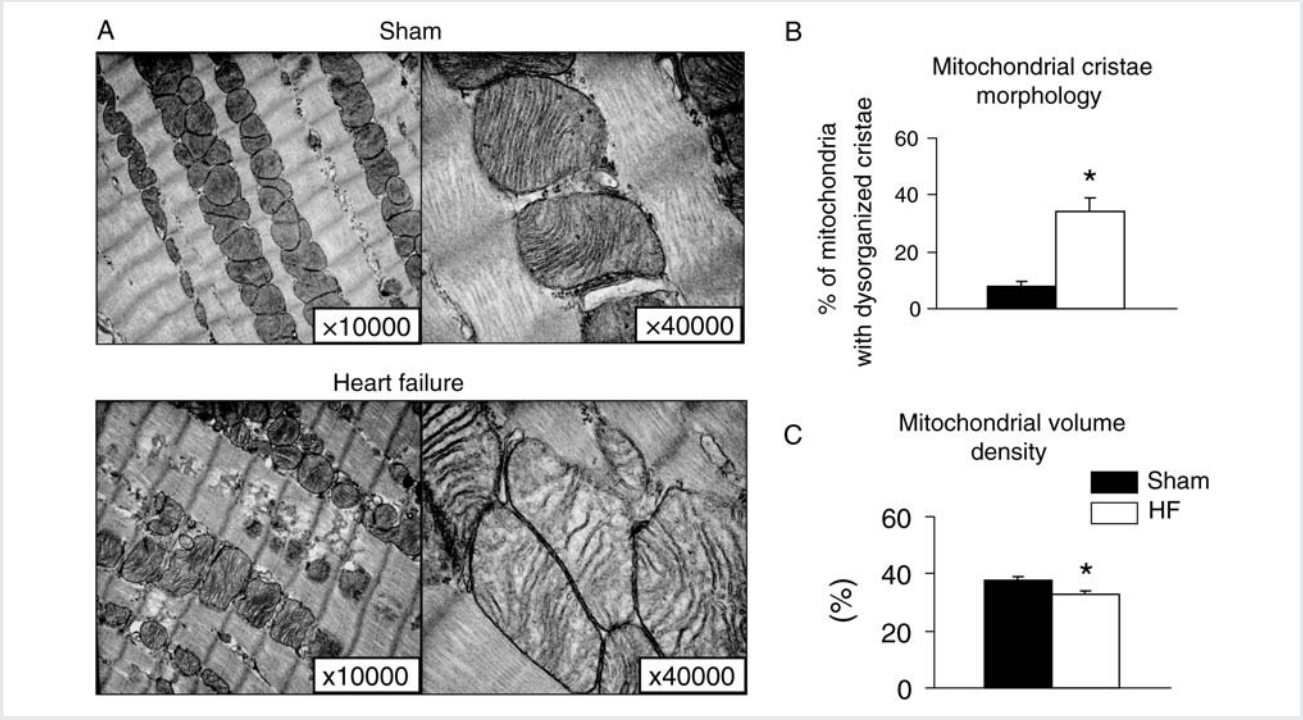

Figure 2 Analysis of cardiac ultrastructure. Representative longitudinal electron microscopy images at a magnification of ×10 000, and ×40 000 (*A*), quantification of changes in mitochondrial cristae morphology (*B*), and quantification of mitochondrial volume density (*C*) of hearts of sham-operated rats (black bars, $n = 3$) and rats with heart failure (white bars, $n = 3$). *$P < 0.05$

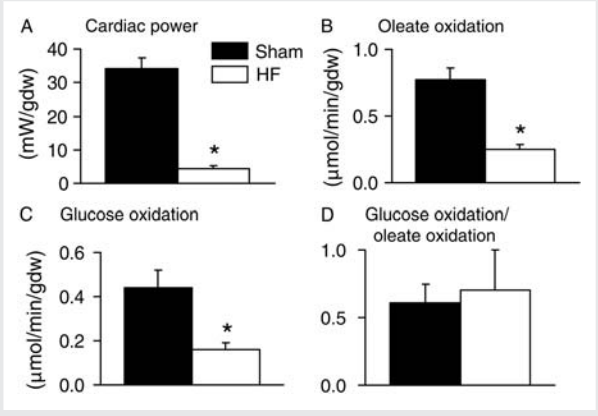

Figure 3 Impaired substrate oxidation in failing hearts. Cardiac power (*A*), oleate oxidation (*B*), glucose oxidation (*C*), and glucose oxidation/oleate oxidation ratio (*D*) of sham-operated rats (black bars, $n = 7$) and rats with heart failure (white bars, $n = 3$) determined in the isolated working heart. *$P < 0.05$.

a similar gene regulatory pattern was observed in non-transgenic mice with hypertrophy following aortic constriction.[32] Other studies also demonstrated reduced expression of PGC-1α and its targets in pathological forms of cardiac hypertrophy and heart failure.[4,33–35] While only one of the two generated lines of PGC-1α knock out mice developed moderate cardiac dysfunction under baseline conditions, Arany *et al.* showed that PGC-1α expression is required for the adaptation of the heart to pressure overload in PGC-1α knockout mice.[32,35,36] A study by Garnier *et al.*[4] showed that mRNA levels of PGC-1α, its targets TFAm and NRF2, as well as the ETC subunit COX4 were downregulated in pressure overload-induced heart failure in rats. Besides heart failure, downregulation of ETC subunits due to reduced PGC-1α levels has also been proposed to contribute to mitochondrial dysfunction in Type 1 diabetic Akita hearts and skeletal muscle in human Type 2 diabetes.[16,23] Thus, the concept is discussed that the downregulation of ETC subunits due to reduced PGC-1α signalling may contribute to oxidative defects in several diseases, including the failing heart, and that an early downregulation of PGC-1α during the development of cardiac hypertrophy may reflect its role as a primary event during the hypertrophic response as opposed to being an indirect consequence of pathological hypertrophy or heart failure.[31,37] Indeed, gene expression of PGC-1α and its target ERRα, which is also a powerful regulator of ETC gene transcription, was associated with reduced mRNA levels of three ETC genes in the present study. In addition, downregulation of PGC-1α was associated with reduced mRNA levels of CPT1, MCAD, and PDK4, all of which can be regulated by PGC-1α.[38,39] However, five ETC genes were not downregulated, and while expression of ETC genes was bidirectional and showed larger differences in mean values, ETC protein subunits encoded by these genes showed only minor changes in abundance. Importantly, only some of the investigated ETC genes were identically regulated on the protein level. Thus, the final contribution of reduced expression of PGC-1α and ERRα to proteomic remodelling in our model of heart failure remains inconclusive.

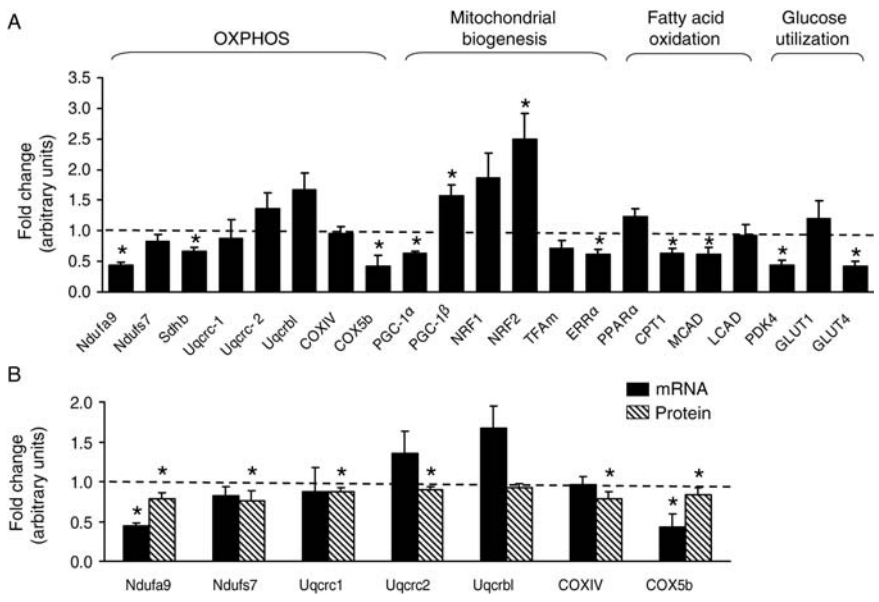

Figure 4 Gene expression profile of failing hearts. Gene expression in failing hearts (*A*), normalized to S29 ribosomal protein transcript levels ($n = 5–8$), and comparison of mRNA levels and mitochondrial protein levels of ETC subunits (*B*). Values represent fold changes relative to WT, which was assigned as 1 (dashed line). $^*P < 0.05$.

Mechanisms of mitochondrial dysfunction independent of changes in protein levels include oxidative stress, which is a well-known condition in failing hearts, and which may compromise ETC complex activity due to oxidative damage, as also occurs in streptozotocin diabetic hearts.[5,6,40] Sparagna *et al.*[7] showed that mitochondrial membrane tetralinoleoyl cardiolipin content is decreased in failing hearts, and cardiolipin is required for full activity of ETC complexes I, III, and IV. Lewandowski's group showed that a defect in TCA cycle anaplerosis may impair mitochondrial substrate oxidation.[8] Studies from Hoppel's group suggest that defects in supermolecular assembly of ETC complexes may limit ETC function in failing hearts.[2] The latter mechanism is of particular interest since minor changes in protein levels may affect appropriate supercomplex formation, and the relative contribution of respirasome formation to electron transport efficiency remains to be elucidated.

A recent proteomics study by Page *et al.*[41] demonstrated downregulation of many mitochondrial proteins in hibernating swine myocardium, including acyl-CoA dehydrogenases and subunits of ETC complexes I, III, and V, suggesting that repetitive events of myocardial ischaemia lead to downregulation of mitochondrial oxidative capacity. Thus, it could be speculated that reduced subendocardial blood flow due to severe cardiac hypertrophy may partially contribute to the downregulation of mitochondrial FAO and ETC proteins in our model. While the extent of downregulation of mitochondrial proteins was on average ~2-fold in hibernating myocardium, downregulation of mitochondrial proteins may be less severe in our model, since we analysed mitochondria obtained from the entire heart, including non-ischaemic cardiac tissue. Studies remain to be conducted to estimate the potential contribution of ischaemic events to mitochondrial proteomic remodelling in pressure overload-induced heart failure.

A possible limitation of our proteomic survey may be the use of trypsin to release mitochondria from cardiac muscle fibres during the isolation procedure. Trypsin has strong proteolytic activity, which was also used to digest protein samples for mass spectrometric analysis in the current study. While we cannot rule out that tryptic treatment of muscle fibres during the isolation process may have resulted in cleavage of proteins, which may have affected peptide quantification by LC-MS/MS, identical tryptic treatment of both groups during mitochondrial isolation may argue against artificial differences in protein levels between the groups.

In conclusion, pressure overload-induced heart failure is characterized by substantial defects in cardiac oxidative capacity. Both fatty acid and glucose oxidation were markedly decreased, accompanied by a mitochondrial defect which likely localizes downstream of substrate-specific pathways. Our proteomic survey suggests that reduced FAO rates may be explained by reduced FAO protein levels. Remodelling of the ETC may also partially contribute to mitochondrial respiratory dysfunction, but other mechanisms are likely to contribute. Our study supports the concept that a global oxidative defect due to mitochondrial dysfunction contributes to the onset and/or severity of cardiac dysfunction following transition of pressure overload hypertrophy to overt heart failure. Future studies should combine comparative proteomics with systematic measurements of intermediate metabolites, i.e. metabolomics, to allow more powerful conclusions on the contribution of proteomic remodelling to altered substrate metabolism.

Supplementary material

Supplementary Material is available at *Cardiovascular Research* online.

Contributions of authors

H.B.: research concept and design, data acquisition (electron microscopy, proteomic experiments), data analysis and interpretation, manuscript preparation. M.S.: data acquisition (real-time PCR, isolation of mitochondria), data analysis, manuscript preparation. D.C.: electron microscopy, proteomic experiments. A.S.: echocardiography, isolation of mitochondria. P.A.A.: surgical intervention, measurement of mitochondrial respiration. M.S.: echocardiography, isolation of mitochondria. T.D.N.: isolated working heart perfusion, statistical analysis. F.W.M.: revision of the manuscript. O.K.: Proteomic experiments. B.C.W.: revision of the manuscript. T.D.: grant holder, supervision, revision of the manuscript.

Conflict of interest: none declared.

Funding

T.D. is Heisenberg Professor of the Deutsche Forschungsgemeinschaft at the University of Leipzig and this work was supported by grants of the Deutsche Forschungsgemeinschaft [Do 602/4-1, 6-1, 8-1]. H.B. was supported by a post-doctoral fellowship grant from the Deutsche Forschungsgemeinschaft [Bu 2126/1-1].

References

1. Bugger H, Chen D, Riehle C, Soto J, Theobald HA, Hu XX *et al.* Tissue-specific remodeling of the mitochondrial proteome in type 1 diabetic Akita mice. *Diabetes* 2009;**58**:1986–1997.
2. Rosca MG, Vazquez EJ, Kerner J, Parland W, Chandler MP, Stanley W *et al.* Cardiac mitochondria in heart failure: decrease in respirasomes and oxidative phosphorylation. *Cardiovasc Res* 2008;**80**:30–39.
3. Lesnefsky EJ, Moghaddas S, Tandler B, Kerner J, Hoppel CL. Mitochondrial dysfunction in cardiac disease: ischemia–reperfusion, aging, and heart failure. *J Mol Cell Cardiol* 2001;**33**:1065–1089.
4. Garnier A, Fortin D, Delomenie C, Momken I, Veksler V, Ventura-Clapier R. Depressed mitochondrial transcription factors and oxidative capacity in rat failing cardiac and skeletal muscles. *J Physiol* 2003;**551**:491–501.
5. Sheeran FL, Pepe S. Energy deficiency in the failing heart: linking increased reactive oxygen species and disruption of oxidative phosphorylation rate. *Biochim Biophys Acta* 2006;**1757**:543–552.
6. Ide T, Tsutsui H, Kinugawa S, Utsumi H, Kang D, Hattori N *et al.* Mitochondrial electron transport complex I is a potential source of oxygen free radicals in the failing myocardium. *Circ Res* 1999;**85**:357–363.
7. Sparagna GC, Chicco AJ, Murphy RC, Bristow MR, Johnson CA, Rees ML *et al.* Loss of cardiac tetralinoleoyl cardiolipin in human and experimental heart failure. *J Lipid Res* 2007;**48**:1559–1570.
8. Sorokina N, O'Donnell JM, McKinney RD, Pound KM, Woldegiorgis G, LaNoue KF *et al.* Recruitment of compensatory pathways to sustain oxidative flux with reduced carnitine palmitoyltransferase I activity characterizes inefficiency in energy metabolism in hypertrophied hearts. *Circulation* 2007;**115**:2033–2041.
9. Murray AJ, Cole MA, Lygate CA, Carr CA, Stuckey DJ, Little SE *et al.* Increased mitochondrial uncoupling proteins, respiratory uncoupling and decreased efficiency in the chronically infarcted rat heart. *J Mol Cell Cardiol* 2008;**44**:694–700.
10. Witt H, Schubert C, Jaekel J, Fliegner D, Penkalla A, Tiemann K *et al.* Sex-specific pathways in early cardiac response to pressure overload in mice. *J Mol Med* 2008; **86**:1013–1024.
11. Rajan S, Williams SS, Jagatheesan G, Ahmed RP, Fuller-Bicer G, Schwartz A *et al.* Microarray analysis of gene expression during early stages of mild and severe cardiac hypertrophy. *Physiol Genomics* 2006;**27**:309–317.
12. Sack MN, Rader TA, Park S, Bastin J, McCune SA, Kelly DP. Fatty acid oxidation enzyme gene expression is downregulated in the failing heart. *Circulation* 1996;**94**: 2837–2842.
13. Barger PM, Kelly DP. PPAR signaling in the control of cardiac energy metabolism. *Trends Cardiovasc Med* 2000;**10**:238–245.
14. Akki A, Smith K, Seymour AM. Compensated cardiac hypertrophy is characterised by a decline in palmitate oxidation. *Mol Cell Biochem* 2008;**311**:215–224.
15. Hanash S. Disease proteomics. *Nature* 2003;**422**:226–232.
16. Mootha VK, Bunkenborg J, Olsen JV, Hjerrild M, Wisniewski JR, Stahl E *et al.* Integrated analysis of protein composition, tissue diversity, and gene regulation in mouse mitochondria. *Cell* 2003;**115**:629–640.
17. Taylor SW, Fahy E, Zhang B, Glenn GM, Warnock DE, Wiley S *et al.* Characterization of the human heart mitochondrial proteome. *Nat Biotechnol* 2003;**21**:281–286.
18. Da Cruz S, Parone PA, Martinou JC. Building the mitochondrial proteome. *Expert Rev Proteomics* 2005;**2**:541–551.
19. Johnson DT, Harris RA, French S, Blair PV, You J, Bemis KG *et al.* Tissue heterogeneity of the mammalian mitochondrial proteome. *Am J Physiol Cell Physiol* 2007; **292**:C689–C697.
20. Boudina S, Bugger H, Sena S, O'Neill BT, Zaha VG, Ilkun O *et al.* Contribution of Impaired myocardial insulin signaling to mitochondrial dysfunction and oxidative stress in the heart. *Circulation* 2009;**119**:1272–1283.
21. Zaha V, Grohmann J, Gobel H, Geibel A, Beyersdorf F, Doenst T. Experimental model for heart failure in rats—induction and diagnosis. *Thorac Cardiovasc Surg* 2003;**51**:211–215.
22. Fischer-Rasokat U, Beyersdorf F, Doenst T. Insulin addition after ischemia improves recovery of function equal to ischemic preconditioning in rat heart. *Basic Res Cardiol* 2003;**98**:329–336.
23. Bugger H, Boudina S, Hu XX, Tuinei J, Zaha VG, Theobald HA *et al.* Type 1 diabetic akita mouse hearts are insulin sensitive but manifest structurally abnormal mitochondria that remain coupled despite increased uncoupling protein 3. *Diabetes* 2008;**57**:2924–2932.
24. Schwarzer M, Faerber G, Rueckauer T, Blum D, Pytel G, Mohr FW *et al.* The metabolic modulators, Etomoxir and NVP-LAB121, fail to reverse pressure overload induced heart failure *in vivo*. *Basic Res Cardiol* 2009;**104**:547–557.
25. Bugger H, Leippert S, Blum D, Kahle P, Barleon B, Marme D *et al.* Subtractive hybridization for differential gene expression in mechanically unloaded rat heart. *Am J Physiol Heart Circ Physiol* 2006;**291**:H2714–H2722.
26. Depre C, Shipley GL, Chen W, Han Q, Doenst T, Moore ML *et al.* Unloaded heart in vivo replicates fetal gene expression of cardiac hypertrophy. *Nat Med* 1998;**4**:1269–1275.
27. Barger PM, Brandt JM, Leone TC, Weinheimer CJ, Kelly DP. Deactivation of peroxisome proliferator-activated receptor-alpha during cardiac hypertrophic growth. *J Clin Invest* 2000;**105**:1723–1730.
28. Neubauer S. The failing heart—an engine out of fuel. *N Engl J Med* 2007;**356**: 1140–1151.
29. Craig EE, Chesley A, Hood DA. Thyroid hormone modifies mitochondrial phenotype by increasing protein import without altering degradation. *Am J Physiol* 1998; **275**:C1508–C1515.
30. Bota DA, Davies KJ. Protein degradation in mitochondria: implications for oxidative stress, aging and disease: a novel etiological classification of mitochondrial proteolytic disorders. *Mitochondrion* 2001;**1**:33–49.
31. Finck BN, Kelly DP. Peroxisome proliferator-activated receptor gamma coactivator-1 (PGC-1) regulatory cascade in cardiac physiology and disease. *Circulation* 2007;**115**:2540–2548.
32. Arany Z, He H, Lin J, Hoyer K, Handschin C, Toka O *et al.* Transcriptional coactivator PGC-1 alpha controls the energy state and contractile function of cardiac muscle. *Cell Metab* 2005;**1**:259–271.
33. Sano M, Izumi Y, Helenius K, Asakura M, Rossi DJ, Xie M *et al.* Menage-a-trois 1 is critical for the transcriptional function of PPARgamma coactivator 1. *Cell Metab* 2007;**5**:129–142.
34. Sano M, Wang SC, Shirai M, Scaglia F, Xie M, Sakai S *et al.* Activation of cardiac Cdk9 represses PGC-1 and confers a predisposition to heart failure. *EMBO J* 2004;**23**:3559–3569.
35. Arany Z, Novikov M, Chin S, Ma Y, Rosenzweig A, Spiegelman BM. Transverse aortic constriction leads to accelerated heart failure in mice lacking PPAR-gamma coactivator 1alpha. *Proc Natl Acad Sci USA* 2006;**103**:10086–10091.
36. Leone TC, Lehman JJ, Finck BN, Schaeffer PJ, Wende AR, Boudina S *et al.* PGC-1alpha deficiency causes multi-system energy metabolic derangements: muscle dysfunction, abnormal weight control and hepatic steatosis. *PLoS Biol* 2005;**3**:e101.
37. Lehman JJ, Kelly DP. Transcriptional activation of energy metabolic switches in the developing and hypertrophied heart. *Clin Exp Pharmacol Physiol* 2002;**29**:339–345.
38. Wende AR, Huss JM, Schaeffer PJ, Giguere V, Kelly DP. PGC-1alpha coactivates PDK4 gene expression via the orphan nuclear receptor ERRalpha: a mechanism for transcriptional control of muscle glucose metabolism. *Mol Cell Biol* 2005;**25**: 10684–10694.
39. Vega RB, Huss JM, Kelly DP. The coactivator PGC-1 cooperates with peroxisome proliferator-activated receptor alpha in transcriptional control of nuclear genes encoding mitochondrial fatty acid oxidation enzymes. *Mol Cell Biol* 2000;**20**: 1868–1876.
40. Lashin OM, Szweda PA, Szweda LI, Romani AM. Decreased complex II respiration and HNE-modified SDH subunit in diabetic heart. *Free Radic Biol Med* 2006;**40**: 886–896.
41. Page B, Young R, Iyer V, Suzuki G, Lis M, Korotchkina L *et al.* Persistent regional downregulation in mitochondrial enzymes and upregulation of stress proteins in swine with chronic hibernating myocardium. *Circ Res* 2008;**102**:103–112.